AGU ADVANCING EARTH AND SPACE SCIENCES

Geophysical Research Letters

RESEARCH LETTER
10.1029/2025GL117342

In-Situ Measurements of Dust Aerosols Transported Into the Lower Stratosphere From a Dust Storm Event

D. Li[1,2], B. Vogel[3], L. Wang[1,4], Z. Bai[1], K. Qie[1], D. Peng[1,4], J. Xu[1,4], Q. Li[1], Z. Yang[3], T. Han[5], S. Wang[5], X. Xu[5], and J. Bian[1,4,6]

[1]Laboratory of Middle Atmosphere and Global Environment Observation, Institute of Atmospheric Physics, Chinese Academy of Sciences, Beijing, China, [2]State Key Laboratory of Atmospheric Environment and Extreme Meteorology, Institute of Atmospheric Physics, Chinese Academy of Sciences, Beijing, China, [3]Institute of Climate and Energy Systems-Stratosphere, Forschungszentrum Jülich, Jülich, Germany, [4]College of Earth and Planetary Sciences, University of Chinese Academy of Sciences, Beijing, China, [5]Golmud Meteorological Bureau, Golmud, China, [6]College of Atmospheric Sciences, Lanzhou University, Lanzhou, China

Key Points:

- Balloon-borne measurements over the Tibetan Plateau reveal enhanced aerosol layer near the tropopause
- Surface area distributions near the tropopause associated with dust storm show bimodal peaks (~0.2 and ~2.21 μm)
- The Middle East and Northern African dust were transported long distances and uplifted into the tropopause region

Correspondence to:
J. Bian,
bjc@mail.iap.ac.cn

Citation:
Li, D., Vogel, B., Wang, L., Bai, Z., Qie, K., Peng, D., et al. (2025). In-situ measurements of dust aerosols transported into the lower stratosphere from a dust storm event. *Geophysical Research Letters*, *52*, e2025GL117342. https://doi.org/10.1029/2025GL117342

Received 3 JUN 2025
Accepted 25 NOV 2025

Author Contributions:
Conceptualization: J. Bian
Data curation: Z. Bai
Formal analysis: J. Bian
Methodology: D. Li
Supervision: J. Bian
Validation: D. Li
Visualization: D. Li
Writing – original draft: D. Li, Q. Li
Writing – review & editing: D. Li, B. Vogel, L. Wang, Z. Bai, K. Qie, D. Peng, J. Xu, Z. Yang, J. Bian

Abstract The vertical distribution of aerosols in the upper troposphere (UT) and lower stratosphere is critical for aerosol-cloud interactions. Balloon-borne measurements in Golmud, over the northern Tibetan Plateau revealed enhanced particle backscatter and number concentrations in the UT and up to 0.5 km above the tropopause on 27 March 2021. The aerosol surface area distribution near the tropopause (12.47 ± 1 km) exhibited bimodal peaks at ~0.2 and ~2.21 μm, differing from the typical unimodal Asian tropopause aerosol layer. Backward trajectory calculations demonstrate that a dust storm over Middle East and northeastern Africa around 24 March transported dust from the lower troposphere to the UT, strongly influencing the observed aerosol profile in Golmud. These results highlight the long-range transport of dust aerosols to the UTLS and their role in modifying vertical aerosol distribution in remote regions.

Plain Language Summary The size distribution of particles in the upper troposphere and lower stratosphere is important for better understanding how aerosols affect climate and cloud formation. Here, balloon-borne instruments (the Compact Optical Backscatter Aerosol Detector and the portable optical particle spectrometer) were used to measure the vertical distribution of particles over Golmud, on the northern Tibetan Plateau. On 27 March 2021, we measured an unusual layer of aerosol in the upper troposphere and lower stratosphere. The aerosols near the tropopause showed a two-peak size pattern, differing from the Asian tropopause aerosol layer with single peak. Based on backward trajectories and satellite measurements, the bimodal distribution was linked to a dust storm in Middle East and northeastern Africa a few days earlier. Our measurements demonstrate that the vertical transport of dust aerosols from the lower troposphere to the tropopause region through long-range transport.

1. Introduction

Aerosols in the upper troposphere and the lower stratosphere (UTLS, ±5 km around the tropopause) exhibit significantly longer atmospheric lifetimes compared to those in the lower troposphere (Deshler, 2008; Hamil et al., 1997; Hirsch & Koren, 2021). Once transported into the UTLS, aerosols can undergo long-range transport driven by large-scale dynamical circulation, influencing Earth's radiation balance and contributing to the direct radiative effect, thereby exerting a notable impact on the climate system (Kok et al., 2017). Dust aerosols is one of the dominant aerosol types in the UTLS (Zhu et al., 2021). These dust aerosols are mainly generated from deserts, including the Sahara, Thar, Taklamakan, and Gobi deserts (Chen et al., 2023). Among these, the Indian Peninsula is the largest source of dust aerosol near the tropopause, followed by the Middle East, together accounting for more than half of the dust observed near the tropopause (Zhu et al., 2021). Dust particles originating from the Taklamakan and Gobi deserts show size-dependent atmospheric transport behaviors: coarse particles typically settle near the surface, while fine particles can ascend to the middle and upper troposphere and be transported over long distances by the prevailing westerly jet (Huang et al., 2008; Xu et al., 2018). Dust aerosols are primary ice nuclei particles involved in cirrus cloud formation (Pan et al., 2019). Dust particles transported into the middle-upper troposphere can act as ice nuclei, contributing to ice cloud formation and thereby indirectly in modulating radiation and precipitation patterns (Creamean et al., 2013). Observational evidence from a high altitude station in Switzerland demonstrated that ice nuclei concentrations increased by one or two orders of magnitude during

Saharan dust events of varying intensities (Brunner et al., 2021). Additionally, dust-veiled cloud layers can be uplifted to altitudes of approximately 8–10 km in the upper troposphere and transported globally (Uno et al., 2009). Furthermore, dust aerosols contribute to atmospheric heating through direct radiative absorption in the middle troposphere (Huang et al., 2009, 2014). Therefore, accurately quantifying the vertical size distribution of dust aerosols is essential for assessing their climatic effects.

Measurements data on the vertical distribution of dust aerosols in the upper troposphere remain limited. Satellite missions such as CALIPSO (Cloud Aerosol LiDAR and Infrared Pathfinder Satellite Observations) have provide valuable insights into the vertical structure of aerosols. While the CALIOP (Cloud Aerosol LiDAR with Orthogonal Polarization) offered dust layers with high vertical resolution, its narrow swath width restricted global spatial coverage. Furthermore, the CALIOP mission ended in August 2023. Furthermore, CALIOP exhibited limited sensitivity to thin aerosols plumes, such as the volcanic plume from the Hunga Tonga eruption, which was observed at ∼24 km over Lijiang, China, using in-situ balloon-borne measurements (Bian et al., 2023). The ground-based LiDAR networks and aircraft platform are indispensable for aerosol monitoring (De Mazière et al., 2018). Lidar-based measurements of stratospheric aerosols have been conducted for nearly five decades, beginning in 1976 (Trickl et al., 2024). The NASA Atmospheric Tomography Mission (ATom) using airborne instruments collected aerosol data from 0.2 to 12 km altitudes over the Pacific and Atlantic oceans from 2016 to 2018 (Froyd et al., 2022). The upper-air aircraft campaign was conducted in South Asia to investigate the Asian Tropopause Aerosol Layer (ATAL) (Vogel et al., 2024). These measurements provided the particle size vertical distributions in the upper troposphere. This study focuses on the UTLS region extending from 5 km below to 5 km above the tropopause.

The Tibetan Plateau, characterized by its strong thermodynamic forcing and elevated terrain, acts as an important pathway for troposphere-to-stratosphere transport (Bian et al., 2020). High dust aerosol optical depth in the upper troposphere has been measured downstream of the Tibetan Plateau based on CALIOP measurements (Xu et al., 2018). Dust aerosols are typically transported to the mid-troposphere over dust source regions and subsequently uplifted to the upper troposphere by prevailing winds over the Tibetan Plateau. Furthermore, fine dust aerosols originating from the Taklamakan Desert can be uplifted into the lower stratosphere via vertical transport processes driven by the convergence of northerly and southerly airflow systems over the Tibetan Plateau (Yang et al., 2014; Zhang et al., 2015).

This study, we explore the vertical size distribution of aerosols in the UTLS under the influence by a dust storm event over the northeastern Africa. First, the measured data was described. Then the vertical characteristics of aerosol backscatter ratio, number concentration, and size-distribution are shown. Last, the trajectory calculations confirm the dust storm contribution.

2. Data and Methods

The Sounding Water vapor, Ozone, and Particle (SWOP) campaign has been conducted by the Institute of Atmospheric Physics, Chinese Academy of Sciences over the Tibetan Plateau during the summer monsoon period (mid-June to early September) from 2009 to 2019 (Bian et al., 2012, 2023; Li et al., 2017; Ma et al., 2022; Yang et al., 2023). To investigate the annual variability of aerosol layers near the tropopause over the Tibetan Plateau, balloons were launched monthly at Golmud (36.48°N, 94.93°E, 2,780 m above sea level (a.s.l.)) from May 2020 to September 2021, and again throughout 2023.

The balloon payloads included an iMet radiosonde, an electrochemical concentration cell (ECC) ozonesonde (Komhyr et al., 1995), a cryogenic frost point hygrometer (CFH) (Vömel et al., 2007, 2016), and a Compact Optical Backscatter Aerosol Detector (COBALD, Switzerland) (Brunamonti et al., 2018; Hanumanthu et al., 2020). The temperature profile obtained from the iMet radiosonde is selected to determine the height of the temperature lapse rate tropopause. According to the World Meteorological Organization (WMO, 1957), the tropopause is defined as "the lowest level at which the lapse rate decreases to 2°C km^{-1} or less, provided also the average lapse rate between this level and all higher levels within 2 km does not exceed 2°C km^{-1}." The backscatter ratio (BSR) from COBALD is retrieved from Equation 1, where β_m is the molecular backscatter coefficient, and β_p is the particle backscatter coefficient. The color index (CI), defined by Equation 2, provides the particle size information. The high CI (>10), relative humidity over ice (RHiFP) from CFH exceeding 70%, and BSR_{940nm} (>∼2) typically indicate the occurrences of large ice particles (Yang et al., 2023). In contrast, aerosol

Table 1
This Study Includes Balloon Launches in Golmud During 2020 and 2021

Date	Instruments	Properties
2 Aug. 2020	ECC + CFH + COBALD + POPS	ATAL
2 Nov. 2020	ECC + CFH + COBALD	BSR (mean)
24 Nov. 2020	ECC + CFH + COBALD + POPS	
22 Dec. 2020	ECC + CFH + COBALD	
2 Feb. 2021	ECC + CFH + COBALD + POPS	
3 Mar. 2021	ECC + CFH + COBALD	
27 Mar. 2021	ECC + CFH + COBALD + POPS	Dust

Note. ECC, electrochemical concentration cell; CFH, cryogenic frost point hygrometer; COBALD, Compact Optical Backscatter Aerosol Detector; POPS, portable optical particle spectrometer; BSR, backscatter ratio; ATAL, Asian Tropopasue Aerosol Layer.

layers are typically identified under cloud-free conditions when BSR_{455nm} is greater than ~1.025 and RHiFP remains below 70% (Brunamonti et al., 2018; Hanumanthu et al., 2020).

$$BSR = \frac{\beta_m + \beta_p}{\beta_m} \quad (1)$$

$$CI = \frac{BSR_{940nm} - 1}{BSR_{455nm} - 1} \quad (2)$$

This study used the COBALD BSR profiles on 2 November, 24 November, 22 December in 2020, 2 February, 3 March, and 27 March in 2021. Additionally, on 2 August, 24 November in 2020, 2 February, 27 March in 2021, a portable optical particle spectrometer (POPS) (Gao et al., 2016) was added to the payloads to investigate aerosol size distributions. More detailed information is provided in Table 1. When data collected via the iMet radiosonde, only 8 discrete bins with diameters (D in μm) of 0.122, 0.144, 0.176, 0.225, 0.416, 0.615, 1.271, 2.055, and 3.394 were available from the POPS instrument. Due to uncertainties associated with instrument errors, the minimum bin (0.122–0.144 μm) was excluded from this analysis. However, if the POPS instrument was recycled, the raw data could be re-binned to higher resolution. In this study, 23 size bins were also used to better resolve and highlight the vertical distribution of particle sizes on 27 March 2021.

The size and surface area distribution (SAD) functions in logarithmic base-10 are defined as follows:

$$\frac{dN}{d\log(D)} = \frac{dN}{dD} \times D \times \ln(10) \quad (3)$$

$$\frac{dA}{d\log(D)} = \frac{dN}{dD} \times \pi \times D^3 \times \ln(10) \quad (4)$$

Where N is the particle number concentration (cm^{-3}), and D is the particle diameter (μm). The size distribution function is typically expressed in units of particles cm^{-3}, while the surface area distribution is expressed in $\mu m^2\ cm^{-3}$.

The CALIOP onboard the CALIPSO was launched on 28 April 2006. The CALIOP level 2 vertical feature mask (VFM) data V4.21 was used in the study. The VFM product provides feature classification including cloud, aerosol, clear sky, and no signal categories (Winker et al., 2013). Tropospheric aerosol subtypes were further distinguished bases on their backscatter signal and depolarization ratio.

The Chemical Lagrangian Model of the Stratosphere (CLaMS) trajectory module (Pommrich et al., 2014; Vogel et al., 2024) was used to calculate backward trajectories along the balloon's ascent track for air parcels over Golmud from the surface to 14 km. Trajectory simulations using CLaMS have previously been applied to investigate transport process over the Asian monsoon anticyclone using ERA5 reanalysis data (Clemens et al., 2024; Li et al., 2020; Vogel et al., 2023) as well as its predecessor ERA-Interim data (Vogel et al., 2015, 2019). The model accounts for isentropic advection, cross-isentropic transport, and vertical mixing, making it well suited for simulating tracer transport in the UTLS. The CLaMS model uses a hybrid vertical coordinate: an isentropic for pressure levels lower than 300 hPa and pressure-based. The model was driven by ERA5 reanalysis data in 1° × 1° horizontal resolution (Hersbach et al., 2020; Hoffmann et al., 2019).

3. Results and Discussion

3.1. Vertical Distribution of Dust Aerosols in the UTLS

Figure 1 shows the vertical distribution of the backscatter ratio measured by COBALD blue (455 nm) and infrared (940 nm) channels, relative to the temperature lapse-rate tropopause (trop: 12.47 km). On 27 March 2021, both the blue and infrared backscatter ratios (Figures 1a and 1b) increased significantly in the upper troposphere compared to the mean value which was calculated based on COBALD measurements on 2 November, 24 November,

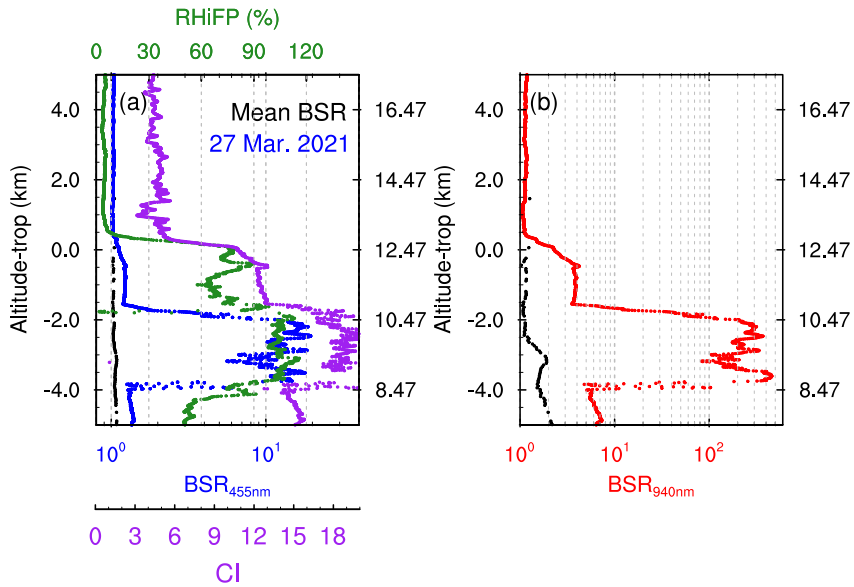

Figure 1. Vertical profiles of particles backscatter ratio (BSR) at 455 nm (a) and 940 nm (b). In (a), relative humidity over ice (RHiFP, green), and color index (CI, purple) along with the tropopause (12.47 km)-relative altitude (Altitude -trop) measured over Golmud on 27 March 2021. The black lines represent the mean backscatter profile at 455 nm (a) and 940 nm (b).

22 December 2020, 2 February, and 3 March 2021. The observed profile on 27 March suggests the occurrence of cirrus clouds in the upper troposphere and 0.5 km above the tropopause over Golmud during spring, with BSR_{940nm} exceeded 2. Identifying aerosols within ice clouds is often challenging when relying solely on COBALD backscatter measurements. However, on this occasion, the POPS instrument was carried out on 27 March 2021 and recycled, provided a unique opportunity to probe aerosol size distributions even within cirrus layers.

The POPS measurements on 27 March 2021 in Golmud also show a significant aerosol layer in the upper troposphere and 0.5 km above the tropopause compared to the profiles observed on 2 August 2020 (the Asian tropopause aerosol layer in Summer), on 24 November 2020 and 2 February 2021 (clear-sky in Spring). The number concentration of particles in the upper troposphere reached approximately 100 cm^{-3}, then decreased with increasing altitude (Figure 2a). The particles number concentration decreased to 50 cm^{-3} near the tropopause, but

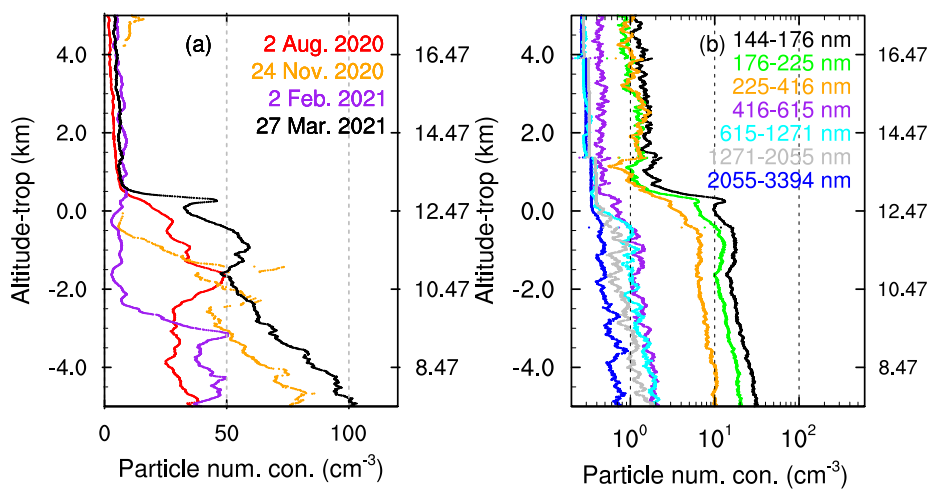

Figure 2. Vertical profiles for aerosol number concentration (a) at Golmud on 2 August 2020, 24 November 2020, 2 February 2021, and 27 March 2021, measured by POPS with the altitude relative to the temperature lapse-rate tropopause. Aerosol size distribution across 7 bins measured by POPS on 27 March 2021 (b).

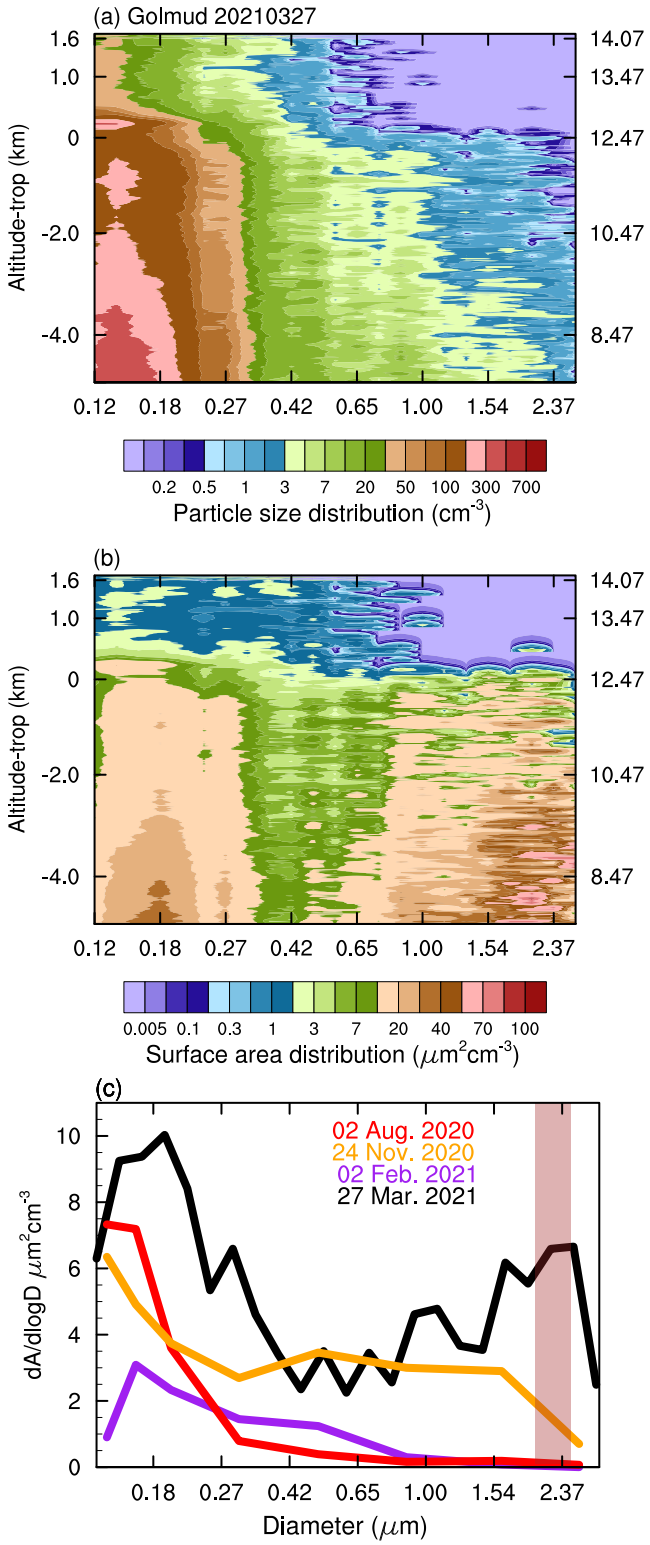

Figure 3.

is slightly higher than the value of 35 cm^{-3} observed at Golmud during the Asian Summer Monsoon period in 2018 (Zhang et al., 2019), but substantially lower than the 180 cm^{-3} at Qaidam in 2019, that was partially influenced by volcanic plume (Zhang et al., 2020). As shown in Figure 2b, the aerosol size distribution in the UTLS was predominantly composed of particles with diameters below 0.416 μm. The particles number concentration in the 0.144–0.176 μm diameter range exceeded 10 cm^{-3} in the upper troposphere, while the concentration of particles larger than 0.416 μm decreased by one order of magnitude. Notably, aerosols with diameter greater than 0.416 μm were present on 27 March 2021, whereas such particles were much less pronounced in previous measurements over Golmud in 2018 (Zhang et al., 2019) and in Qaidam Basin, approximately 190 km the north-northeast of Golmud in 2019 (Zhang et al., 2020).

To investigate the finer-scale structure of particles, Figures 3a and 3b show the vertical distribution of particle number concentration and surface area distribution function across 23 size bins on 27 March 2021 over Golmud. The number concentration distribution of particles from 5.0 km below the tropopause to 0.5 km above the tropopause showed a maximum value of 500 cm^{-3} around 4.5 km below the tropopause in the vertical direction and showed a single size peak located between 0.12 and 0.21 μm across the 23 size bins. In contrast, the SAD showed a bimodal structure. Besides the fine particle peak between 0.12 and 0.21 μm, an additional peak appeared around 2.21 μm (Figure 3b) in the upper troposphere and 0.5 km above the tropopause. Figure 3c further shows the surface area distribution as a function of particle diameter for the 2-km layer: 1 km above and 1 km below the tropopause. The surface area distribution function near the tropopause on 27 March 2021 over Golmud showed two distinct peaks—-one centered around 0.2 μm and another around 2.21 μm. Whereas the Asian tropopause aerosol layer featured only a signal dominant peak less than 0.18 μm on 2 August 2020. Two other cases observed by POPS on 24 November 2020 and on 2 February 2021 under the clean-sky condition in Golmud show the distributions, with the values much lower than those observed on 27 March 2021. Implying that the particles on 27 March in Golumd possible have additional source regions.

3.2. Dust Aerosol Transported Into the Lower Stratosphere Following a Dust Storm Event

In order to investigate the source region of aerosols from surface to 14 km over Golmud, Figures 4a and 4b show the 5-day backward trajectories for air particles originating from the altitude below 3.5 km. The CLaMS backward trajectories indicates that particles in Golmud pass through the Taklamakan desert on 26 March at altitude 7–12 km, and then could be traced to the Middle East and northeastern Africa on 22–24 March in the lower troposphere below 3.5 km. The trajectories show that air parcels passed over the

Figure 3. Vertical distribution of aerosol size distribution (a), surface area distribution (b) across 23 size bins measured at Golmud on 27 March 2021. The vertical axis shows altitude relative to the tropopause. The mean surface area distribution for the layers extending from 1 km below to 1 km above the tropopause (c) as a function of particle diameter. On 2 August, the Asian tropopause aerosol layer (red), 24 November 2020 (orange), and 2 March 2021 (purple) mark the surface area distributions in Golmud under clear sky conditions. *X*-axis is on a logarithmic scale. The brown polygon marks the coarse particle peak.

10.1029/2025GL117342

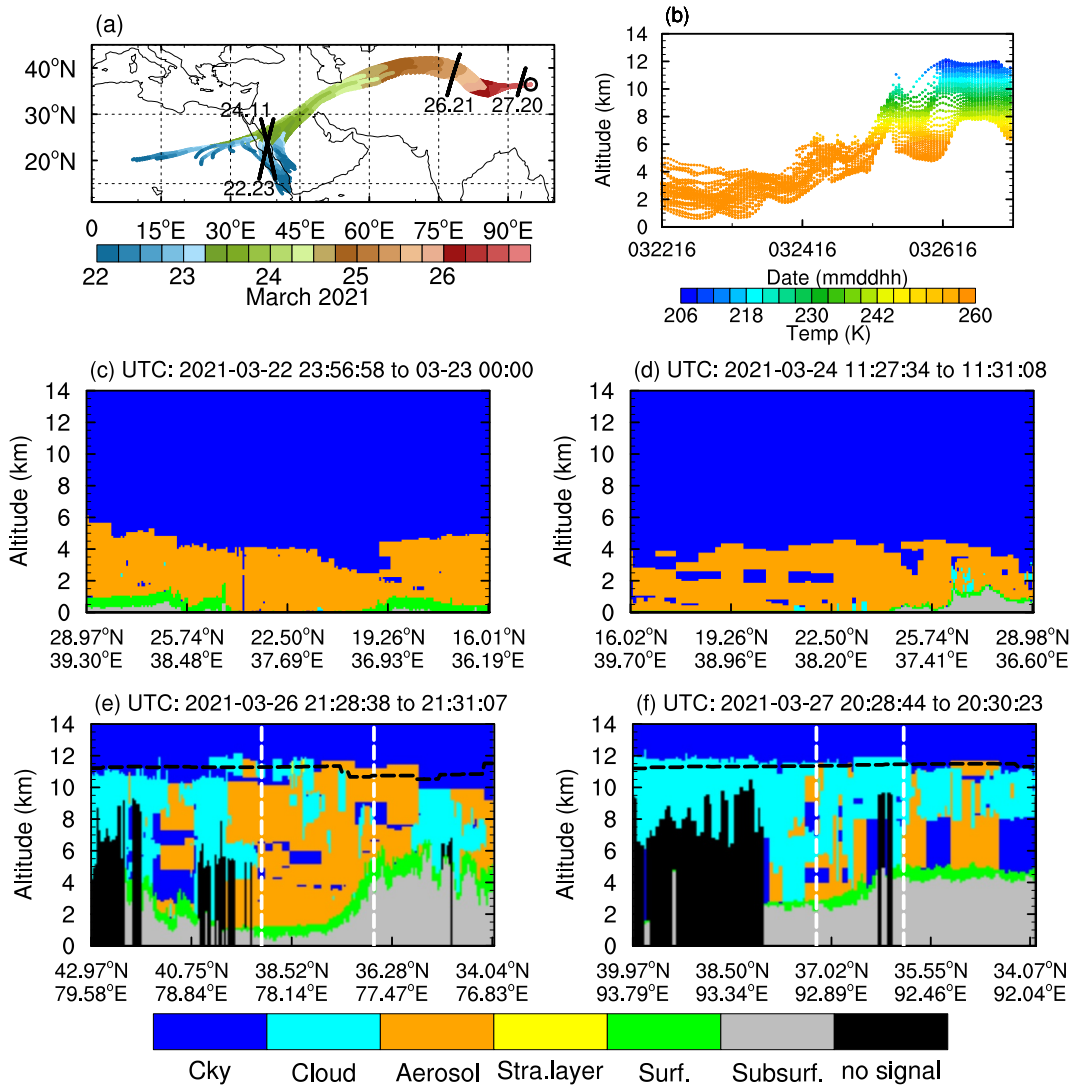

Figure 4. The 5-day backward trajectories for air parcels at Golmud (a). The black line marks the orbit track of the CALIPSO on 22 March at ~23:58 UTC (22.23), on 24 March at ~11:29 UTC (24.11), 26 March at ~21:30 UTC (26.21), and on 27 March at ~20:29 UTC (27.20). Vertical feature mask from CALIOP measurements along the tracks shown on 22 March (c), 24 March (d), 26 March (e), and 27 March (f). Cky: clear sky, Cloud, Aerosol: aerosol (subtype: dust), Stra.layer: stratospheric aerosol, Surf: Surface, Subsurf: subsurface, and no signal. The vertical dashed lines mark the latitude air parcels pass through. The horizontal dashed lines mark the temperature lapse tropopause.

Taklamakan desert region with weak ascent above 7 km on 26 March at 16:00-22:00 (Figure 4b), suggesting limited uplift process below 7 km. In contrast, a significant ascent process from 5 to 10 km is simulated over the Iranian Plateau.

Previous studies have demonstrated that dust aerosols originating from the Middle East and northern Africa can transport long-range distance in the troposphere, probably acting as ice nuclei and playing a key role in could formation and precipitation (Creamean et al., 2013; Froyd et al., 2022; Yu et al., 2017). The VFM from CALIOP on 22, 24, 26, and 27 March 2021 (Figures 4c–4f) confirmed the occurrence of a dust storm over the northeastern Africa and Middle East on 22–24 March and the Taklamakan desert on 26 March measured in Golmud by COBALD and POPS. The CALIPSO VFM overpass on 26 March, one day prior to the POPS measurements on 27 March, clearly shows the vertical structure of dust from the surface to ~12 km altitude and dust-veiled clouds near the tropopause around 37–39°N over the Taklamakan Desert. Dust aerosols from the northeastern Africa and Middle East desert can be transported over long-range distances under the influence of

southwesterly wind flow, then be uplifted into the middle and upper troposphere while passing over the Iranian Plateau and the Tibetan Plateau (Eguchi et al., 2009; Uno et al., 2009). The troposphere-to-stratosphere transport processes provide a potential pathway for dust aerosols in the upper troposphere to reach altitudes above the thermal tropopause. Both POPS and COBALD instruments captured this tiny signal above the tropopause in Golmud.

4. Conclusions

In this study, balloon-borne measurements of particles backscatter ratio (BSR) and number concentration over Golmud, on the northern Tibetan Plateau in 2020 and 2021 were used to investigate the vertical distribution of aerosols in the UTLS. The observations show that BSR and aerosols concentration in the upper troposphere significantly increased on 27 March 2021. Notably, the number concentration of particles (50 cm^{-3}) near the tropopause on 27 March was higher than that typically observed during the Asian tropopause aerosol layer in Summer. In addition, the surface area distribution showed a bimodal size distribution near the tropopause region: one at approximately 0.2 μm, another at 2.21 μm. The bimodal structure differs from the SAD pattern associated with the Asian tropopause aerosol layer with unimodal, highlighting the unique characteristics of aerosol transport in spring over the Golmud.

CLaMS backward trajectories and CALIOP VFM measurements reveal that dust particles from the Middle East and northeastern Africa is transported over long-range distances, uplifted to the upper troposphere over the Iranian and Tibetan Plateaus. Subsequently, troposphere-to-stratosphere transport serves as a pathway for particles to enter the lower stratosphere (0.5 km above the temperature lapse tropopause). The spring dust near the tropopause over the northern Tibetan Plateau originated from the Middle East and northeastern Africa—the dominant source for the tropopause dust aerosol layer (Zhu et al., 2021). Our findings provide direct observational evidence of the vertical transport pathway, which is critical for improving the representation in climate and chemical transport models.

Conflict of Interest

The authors declare no conflicts of interest relevant to this study.

Data Availability Statement

The data sets used here are publicly available as follows: The measurements data to produce the figures in the manuscript can be downloaded at Li et al. (2025).

Acknowledgments

This work was partially supported by the National Natural Science Foundation of China (Grant 42394121). The 2021 Golmud observation was greatly supported by the joint NSFC-DFG 2020 project (NSFC Grant 42061134012). The authors gratefully acknowledge the Jülich Supercomputing Center (JSC; Research Centre Jülich, Germany) for the computing time on the supercomputer JUWELS (project CLaMS-ESM) and for the storage resources on the meteocloud data archive. We thank for the technical support of the National Large Scientific and Technological Infrastructure "Earth System Numerical Simulation Facility" (https://cstr.cn/31134.02.EL). The CALIOP data were obtained from the NASA Langley Research Center Atmos pheric Science Data Center. The presented work includes contributions to the NSFC-DFG 2020 project VO 1276/6-1. We thank Xiaolu Yan and Xiangdong Zheng for their participation in the experiment conducted in summer 2020.

References

Bian, J., Li, D., Bai, Z., Li, Q., Lyu, D., & Zhou, X. (2020). Transport of Asian surface pollutants to the global stratosphere from the Tibetan Plateau region during the Asian summer monsoon. *National Science Review*, *7*(3), 516–533. https://doi.org/10.1093/nsr/nwaa005

Bian, J., Li, D., Bai, Z., Xu, J., Li, Q., Wang, H., et al. (2023). First detection of aerosols of the Hunga Tonga eruption in the Northern Hemisphere stratospheric westerlies. *Science Bulletin*, *68*(6), 574–577. https://doi.org/10.1016/j.scib.2023.03.002

Bian, J., Pan, L. L., Paulik, L., Vömel, H., Chen, H., & Lu, D. (2012). In situ water vapor and ozone measurements in Lhasa and Kunming during the Asian summer monsoon. *Geophysical Research Letters*, *39*(19), L19808. https://doi.org/10.1029/2012GL052996

Brunamonti, S., Jorge, T., Oelsner, P., Hanumanthu, S., Singh, B. B., Kumar, K. R., et al. (2018). Balloon-borne measurements of temperature, water vapor, ozone and aerosol backscatter on the southern slopes of the Himalayas during StratoClim 2016–2017. *Atmospheric Chemistry and Physics*, *18*(21), 15937–15957. https://doi.org/10.5194/acp-18-15937-2018

Brunner, C., Brem, B. T., Collaud Coen, M., Conen, F., Hervo, M., Henne, S., et al. (2021). The contribution of Saharan dust to the ice-nucleating particle concentrations at the high altitude station Jungfraujoch (3580 m a.s.l.), Switzerland. *Atmospheric Chemistry and Physics*, *21*(23), 18029–18053. https://doi.org/10.5194/acp-21-18029-2021

Chen, S., Zhao, D., Huang, J., He, J., Chen, Y., Chen, J., et al. (2023). Mongolia contributed more than 42% of the dust concentrations in northern China in March and April 2023. *Advances in Atmospheric Sciences*, *40*(9), 1549–1557. https://doi.org/10.1007/s00376-023-3062-1

Clemens, J., Vogel, B., Hoffmann, L., Griessbach, S., Thomas, N., Fadnavis, S., et al. (2024). A multi-scenario Lagrangian trajectory analysis to identify source regions of the Asian tropopause aerosol layer on the Indian subcontinent in August 2016. *Atmospheric Chemistry and Physics*, *24*(1), 763–787. https://doi.org/10.5194/acp-24-763-2024

Creamean, J. M., Suski, K. J., Rosenfeld, D., Cazorla, A., DeMott, P. J., Sullivan, R. C., et al. (2013). Dust and biological aerosols from the Sahara and Asia influence precipitation in the western U.S. *Science*, *339*(6127), 1572–1578. https://doi.org/10.1126/science.1227279

De Mazière, M., Thompson, A. M., Kurylo, M. J., Wild, J. D., Bernhard, G., Blumenstock, T., et al. (2018). The Network for the Detection of Atmospheric Composition Change (NDACC): History, status and perspectives. *Atmospheric Chemistry and Physics*, *18*(7), 4935–4964. https://doi.org/10.5194/acp-18-4935-2018

Deshler, T. (2008). A review of global stratospheric aerosol: Measurements, importance, life cycle, and local stratospheric aerosol. *Atmospheric Research*, *90*(2–3), 223–232. https://doi.org/10.1016/j.atmosres.2008.03.016

Eguchi, K., Uno, I., Yumimoto, K., Takemura, T., Shimizu, A., Sugimoto, N., & Liu, Z. (2009). Trans-Pacific dust transport: Integrated analysis of NASA/CALIPSO and a global aerosol transport model. *Atmospheric Chemistry and Physics*, *9*, 3137–3145. https://doi.org/10.5194/acp-9-3137-2009

Froyd, K. D., Yu, P., Schill, G. P., Brock, C. A., Kupc, A., Williamson, C. J., et al. (2022). Dominant role of mineral dust in cirrus cloud formation revealed by global-scale measurements. *Nature Geoscience*, *15*(3), 177–183. https://doi.org/10.1038/s41561-022-00901-w

Gao, R. S., Telg, H., McLaughlin, R. J., Ciciora, S. J., Watts, L. A., Richardson, M. S., et al. (2016). A light-weight, high-sensitivity particle spectrometer for PM2.5 aerosol measurements. *Aerosol Science and Technology*, *50*(1), 88–99. https://doi.org/10.1080/02786826.2015.1131809

Hamill, P., Jensen, E. J., Russell, P. B., & Bauman, J. J. (1997). The life cycle of stratospheric aerosol particles. *Bulletin of the American Meteorological Society*, *78*(7), 1395–1410. https://doi.org/10.1175/1520-0477(1997)078<1395:TLCOSA>2.0.CO;2

Hanumanthu, S., Vogel, B., Müller, R., Brunamonti, S., Fadnavis, S., Li, D., et al. (2020). Strong day-to-day variability of the Asian Tropopause Aerosol Layer (ATAL) in August 2016 at the Himalayan foothills. *Atmospheric Chemistry and Physics*, *20*(22), 14273–14302. https://doi.org/10.5194/acp-20-14273-2020

Hersbach, H., Bell, B., Berrisford, P., Hirahara, S., Horànyi, A., Muñoz Sabater, J., et al. (2020). The ERA5 global reanalysis. *Quarterly Journal of the Royal Meteorological Society*, *146*(730), 1999–2049. https://doi.org/10.1002/qj.3803

Hirsch, E., & Koren, I. (2021). Record-breaking aerosol levels explained by smoke injection into the stratosphere. *Science*, *371*(6535), 1269–1274. https://doi.org/10.1126/science.abe1415

Hoffmann, L., Günther, G., Li, D., Stein, O., Wu, X., Griessbach, S., et al. (2019). From ERA-interim to ERA5: The considerable impact of ECMWF's next-generation reanalysis on Lagrangian transport simulations. *Atmospheric Chemistry and Physics*, *19*(5), 3097–3124. https://doi.org/10.5194/acp-19-3097-2019

Huang, J., Fu, Q., Su, J., Tang, Q., Minnis, P., Hu, Y., et al. (2009). Taklimakan dust aerosol radiative heating derived from CALIPSO observations using the Fu-Liou radiation model with CERES constraints. *Atmospheric Chemistry and Physics*, *9*(12), 4011–4021. https://doi.org/10.5194/acp-9-4011-2009

Huang, J., Minnis, P., Chen, B., Huang, Z., Liu, Z., Zhao, Q., et al. (2008). Long-range transport and vertical structure of Asian dust from CALIPSO and surface measurements during PACDEX. *Journal of Geophysical Research*, *113*(D23), D23212. https://doi.org/10.1029/2008JD010620

Huang, J., Wang, T., Wang, W., Li, Z., & Yan, H. (2014). Climate effects of dust aerosols over East Asian arid and semiarid regions. *Journal of Geophysical Research: Atmospheres*, *119*(19), 11398–11416. https://doi.org/10.1002/2014JD021796

Kok, J. F., Ridley, D. A., Zhou, Q., Miller, R. L., Zhao, C., Heald, C. L., et al. (2017). Smaller desert dust cooling effect estimated from analysis of dust size and abundance. *Nature Geoscience*, *10*(4), 274–278. https://doi.org/10.1038/ngeo2912

Komhyr, W. D., Barnes, R. A., Brothers, G. B., Lathrop, J. A., & Opperman, D. P. (1995). Electrochemical concentration cell ozonesonde performance evaluation during STOIC 1989. *Journal of Geophysical Research*, *100*(D5), 9231–9244. https://doi.org/10.1029/94JD02175

Li, D., Vogel, B., Bian, J., Müller, R., Pan, L. L., Günther, G., et al. (2017). Impact of typhoons on the composition of the upper troposphere within the Asian summer monsoon anticyclone: The SWOP campaign in Lhasa 2013. *Atmospheric Chemistry and Physics*, *17*(7), 4657–4672. https://doi.org/10.5194/acp-17-4657-2017

Li, D., Vogel, B., Müller, R., Bian, J., Günther, G., Ploeger, F., et al. (2020). Dehydration and low ozone in the tropopause layer over the Asian monsoon caused by tropical cyclones: Lagrangian transport calculations using ERA-interim and ERA5 reanalysis data. *Atmospheric Chemistry and Physics*, *20*(7), 4133–4152. https://doi.org/10.5194/acp-20-4133-2020

Li, D., Vogel, B., Wang, L., Bai, Z., Qie, K., Peng, D., et al. (2025). In-situ measurements of dust aerosols transported into the lower stratosphere from a dust storm event [Dataset]. *Zenodo*. https://doi.org/10.5281/zenodo.15583788

Ma, D., Bian, J., Li, D., Bai, Z., Li, Q., Zhang, J., et al. (2022). Mixing characteristics within the tropopause transition layer over the Asian summer monsoon region based on ozone and water vapor sounding data. *Atmospheric Research*, *271*, 106093. https://doi.org/10.1016/j.atmosres.2022.106093

Pan, H., Wang, M., Kumar, K. R., Lu, H., Mamtimin, A., Huo, W., et al. (2019). Seasonal and vertical distributions of aerosol type extinction coefficients with an emphasis on the impact of dust aerosol on the microphysical properties of cirrus over the Taklimakan desert in Northwest China. *Atmospheric Environment*, *203*, 216–227. https://doi.org/10.1016/j.atmosenv.2019.02.004

Pommrich, R., Müller, R., Grooß, J.-U., Konopka, P., Ploeger, F., Vogel, B., et al. (2014). Tropical troposphere to stratosphere transport of carbon monoxide and long-lived trace species in the chemical Lagrangian Model of the Stratosphere (CLaMS). *Geoscientific Model Development*, *7*(6), 2895–2916. https://doi.org/10.5194/gmd-7-2895-2014

Trickl, T., Vogelmann, H., Fromm, M. D., Jäger, H., Perfahl, M., & Steinbrecht, W. (2024). Measurement report: Violent biomass burning and volcanic eruptions—A new period of elevated stratospheric aerosol over central Europe (2017 to 2023) in a long series of observations. *Atmospheric Chemistry and Physics*, *24*(3), 1997–2021. https://doi.org/10.5194/acp-24-1997-2024

Uno, I., Eguchi, K., Yumimoto, K., Takemura, T., Shimizu, A., Uematsu, M., et al. (2009). Asian dust transported one full circuit around the globe. *Nature Geoscience*, *2*(8), 557–560. https://doi.org/10.1038/ngeo583

Vogel, B., Günther, G., Müller, R., Grooß, J.-U., & Riese, M. (2015). Impact of different Asian source regions on the composition of the Asian monsoon anticyclone and of the extratropical lowermost stratosphere. *Atmospheric Chemistry and Physics*, *15*(23), 13699–13716. https://doi.org/10.5194/acp-15-13699-2015

Vogel, B., Müller, R., Günther, G., Spang, R., Hanumanthu, S., Li, D., et al. (2019). Lagrangian simulations of the transport of young air masses to the top of the Asian monsoon anticyclone and into the tropical pipe. *Atmospheric Chemistry and Physics*, *19*(9), 6007–6034. https://doi.org/10.5194/acp-19-6007-2019

Vogel, B., Volk, C. M., Wintel, J., Lauther, V., Clemens, J., Grooß, J.-U., et al. (2024). Evaluation of vertical transport in ERA5 and ERA-interim reanalysis using high-altitude aircraft measurements in the Asian summer monsoon 2017. *Atmospheric Chemistry and Physics*, *24*(1), 317–343. https://doi.org/10.5194/acp-24-317-2024

Vogel, B., Volk, C. M., Wintel, J., Lauther, V., Müller, R., Patra, P. K., et al. (2023). Reconstructing high-resolution in-situ vertical carbon dioxide profiles in the sparsely monitored Asian monsoon region. *Communications Earth & Environment*, *4*(1), 72. Article 25. https://doi.org/10.1038/s43247-023-00725-5

Vömel, H., David, D. E., & Smith, K. (2007). Accuracy of tropospheric and stratospheric water vapor measurements by the cryogenic frost point hygrometer: Instrumental details and observations. *Journal of Geophysical Research*, *112*, D08305. https://doi.org/10.1029/2006JD007224

Vömel, H., Naebert, T., Dirksen, R., & Sommer, M. (2016). An update on the uncertainties of water vapor measurements using cryogenic frost point hygrometers. *Atmospheric Measurement Techniques*, *9*(8), 3755–3768. https://doi.org/10.5194/amt-9-3755-2016

Winker, D. M., Tackett, J. L., Getzewich, B. J., Liu, Z., Vaughan, M. A., & Rogers, R. R. (2013). The global 3-D distribution of tropospheric aerosols as characterized by CALIOP. *Atmospheric Chemistry and Physics*, *13*(6), 3345–3361. https://doi.org/10.5194/acp-13-3345-2013

WMO. (1957). Meteorology-A three-dimensional science: Second session of the commission for aerology. *WMO Bull*, *6*(4), 134–138.

Xu, C., Ma, Y., Yang, K., & You, C. (2018). Tibetan Plateau impacts on global dust transport in the upper troposphere. *Journal of Climate*, *31*(12), 4745–4756. https://doi.org/10.1175/JCLI-D-17-0313.1

Yang, Q., Tian, W., Long, X., Chen, L., Zhang, J., Huang, Q., et al. (2014). Transport of dust aerosols from troposphere to stratosphere over Qinghai-Xizang Plateau. *Plateau Meteorology*, *33*, 887–899.

Yang, Z., Li, D., Luo, J., Tian, W., Bai, Z., Li, Q., et al. (2023). Determination of cirrus occurrence and distribution characteristics over the Tibetan Plateau based on the SWOP campaign. *Journal of Geophysical Research: Atmospheres*, *128*(8), e2022JD037682. https://doi.org/10.1029/2022JD037682

Yu, P. F., Rosenlof, K. H., Liu, S., Telg, H., Thornberry, T. D., Rollins, A. W., et al. (2017). Efficient transport of tropospheric aerosol into the stratosphere via the Asian summer monsoon anticyclone. *Proceedings of the National Academy of Sciences of the United States of America*, *114*(27), 6972–6977. https://doi.org/10.1073/pnas.1701170114

Zhang, J., Tian, W., Long, X., Tian, H., Huang, Q., Xu, P., et al. (2015). Fact and simulation of dust aerosol transported to stratosphere during a strong dust storm in South Xinjiang. *Plateau Meteorology*, *34*, 991–1004. (in Chinese). https://doi.org/10.7522/j.issn.1000-0534.2014.00103

Zhang, J., Wu, X., Liu, S., Bai, Z., Xia, X., Chen, B., et al. (2019). In situ measurements and backward-trajectory analysis of high-concentration, fine-mode aerosols in the UTLS over the Tibetan Plateau. *Environmental Research Letters*, *14*(12), 124068. https://doi.org/10.1088/1748-9326/ab5a9f

Zhang, J., Wu, X., Liu, S., Bai, Z., Xia, X., Chen, B., et al. (2020). Aerosol variations in the upper troposphere and lower stratosphere over the Tibetan Plateau. *Environmental Research Letters*, *15*(9), 094068. https://doi.org/10.1088/1748-9326/ab9b43

Zhu, Q., Liu, Y., Shao, T., Luo, R., & Tan, Z. (2021). A simulation study on the new transport pathways of global tropopause dust layer. *Geophysical Research Letters*, *48*(22), e2021GL096063. https://doi.org/10.1029/2021GL096063